A unified transformation function for lower and upper bounding constraints on model parameters in electrical and electromagnetic inversion

2011 J. Geophys. Eng. 8 21

(http://iopscience.iop.org/1742-2140/8/1/004)

IOP PUBLISHING JOURNAL OF GEOPHYSICS AND ENGINEERING
J. Geophys. Eng. **8** (2011) 21–26 doi:10.1088/1742-2132/8/1/004

A unified transformation function for lower and upper bounding constraints on model parameters in electrical and electromagnetic inversion

Hee Joon Kim[1] **and YoungHee Kim**[2]

[1] Department of Energy Resources Engineering, Pukyong National University, Busan 608-737, Korea
[2] Seismological Laboratory, California Institute of Technology, Pasadena, CA 91125, USA

E-mail: ykim@gps.caltech.edu

Received 3 July 2010
Accepted for publication 27 October 2010
Published 1 December 2010
Online at stacks.iop.org/JGE/8/21

Abstract
Since many geophysical inverse problems are ill-posed, implementation of model parameter constraints is important in reducing solution ambiguity. This paper presents a unified transformation function for enforcing lower and upper bounds on model parameters to restrict model updates during the inversion process such that unrealistic results are suppressed. The transformation is realized using a logarithmic or inverse hyperbolic tangent function on model parameters, and contains the conventional transformations as special cases. It is straightforward to recast the cost functional gradient in terms of the transformed variable. The interval between lower and upper bounds reflects the reliability of *a priori* information, which may be obtained from well logging and surface geological surveys. Tests on a synthetic crosswell electromagnetic example reveal that the use of bound constraints is effective in deriving valid physical results from inversion.

Keywords: *a priori* information, constraint, inverse problems

1. Introduction

Geophysical inversion is an ill-posed problem because its solution is neither unique nor stable. This is mainly attributed to an insufficient amount of data collected. In an ill-posed problem, unrealistic models can be found that produce acceptable fits between the observations and predicted data. Regularization techniques are usually utilized to relieve the ill-posed nature of inverse problems (Tikhonov and Arsenin 1977, Constable *et al* 1987).

Implementation of model constraints is helpful in reducing solution ambiguity in the imaging process and avoiding non-physical model parameter estimates. In electrical and electromagnetic (EM) problems, for instance, the logarithm of electrical conductivity (reciprocal of resistivity) is usually used instead of conductivity itself to obtain a stable inverse (e.g. Constable *et al* 1987, Mackie and Madden 1993, Newman and Alumbaugh 2000). The inversion of electrical and EM data recovers logarithmic parameters, allowing for a wide range of the original parameters as well as imposing positivity, which is a physical requirement for conductivity (e.g. Mackie and Madden 1993).

In practice, we often have access to useful information through several ways such as well logging and surface geological and geophysical surveys. Information obtained from these manners is *a priori* estimates about the physical properties of underground regions. Since these are just estimates, their values are only known within a certain range. Kim *et al* (1999) introduced a logarithmic transformation on model parameters to restrict resistivity within an imaging volume to be bounded instead of using log resistivity. Pedersen (2004) and Kim *et al* (1999) employed the logarithmic transformation for their one- and two-dimensional inversions of magnetotelluric data, respectively. Cardarelli and

Fischanger (2006) applied the same technique successfully to electrical resistivity tomography.

Recently, in addition to the logarithmic transformation, Commer and Newman (2008) introduced an inverse hyperbolic tangent transformation to map bounded conductivity parameters to an unbounded domain in the transform space. They demonstrated that these transformations are valuable for inverting marine controlled-source EM (CSEM) data to avoid conductivity overshoots (Gibbs phenomenon) near structural boundaries, which are prone to occur in unbounded inversions. Ueda and Zhdanov (2009) also applied the logarithmic transformation to their marine CSEM inversion based on the regularized conjugate gradient method and EM migration. Thus, inversion routines that allow for lower and upper bounds of model parameters can be quite useful for the final reconstruction.

This paper presents a unified expression for lower and upper bounding constraints on model parameters after reviewing the conventional logarithmic and inverse hyperbolic tangent transformations. The unified formula has another form of logarithmic or inverse hyperbolic tangent transformation, and contains the conventional transformations as its special cases. We then derive the cost functional gradient and model updating formula in terms of the transformed variable. Finally, the new transformation function is incorporated into a regularized Gauss–Newton method and tested on a synthetic crosswell EM example.

2. Conventional bound constraints

The use of proper model parameter constraints is effective in reducing solution ambiguity in the imaging process and avoiding non-physical conductivity estimates, that is, negative or extremely high conductivity estimates. Kim *et al* (1999) proposed inequality constraints to restrict conductivity within an imaging volume to be bounded. Specifically, one requires $a_k < m_k < b_k$ for the kth model parameter m_k, where a_k and b_k are the lower and upper limits, respectively. The transforming method for enforcing lower and upper bounds of model parameters is expressed as

$$x_k = \ln\left(\frac{m_k - a_k}{b_k - m_k}\right), \tag{1}$$

where x_k is the representation of the model component in the transform space. This transformation function is a kind of logistic sigmoid function, which finds applications in a range of fields such as artificial neural networks, biology, economics, probability and statistics. When using the transformation, it is understood that a regularization operator is applied directly to the transformed unknowns, x_k ($k = 1,\ldots, K$), in the minimization procedure. Kim *et al* (1999), Cardarelli and Fischanger (2006) and Song and Kim (2008) applied equation (1) to their inversion procedures based on an iterative smoothness-constrained least-squares algorithm, while Pedersen (2004) applied it to his truncated singular-value decomposition technique. In equation (1), m_k, a_k and b_k are not restricted to positive values unlike the log conductivity (Kim *et al* 1999). This means that the use of bound constraints has a wider range of application fields.

Recently, two different nonlinear transformations were introduced to impose *a priori* information of minimum and maximum bounds on unknown parameters by Commer and Newman (2008) and Abubakar *et al* (2008). The former utilize a hyperbolic tangent function as

$$m_k = \frac{b_k - a_k}{2}\tanh(x_k) + \frac{a_k + b_k}{2}, \tag{2}$$

while the latter employ exponential functions as

$$m_k = \frac{b_k \exp(x_k) + a_k \exp(-x_k)}{\exp(x_k) + \exp(-x_k)}. \tag{3}$$

Commer and Newman (2008) used both equations (1) and (2) for nonlinear conjugate gradient inversion of marine CSEM data, while Abubakar *et al* (2008) employed equation (3) for regularized Gauss–Newton inversion of EM data. As we will see in the next section, equations (2) and (3) are the same, and all three transformations can be merged into a single one.

3. New bound constraints

In this paper, we propose a unified formula for lower and upper bounds of model parameters. It is first expressed by a logarithmic transformation on model parameters as

$$x = \frac{1}{n}\ln\left(\frac{m - a}{b - m}\right) \qquad a < m < b, \tag{4}$$

where n is a positive constant. For simplicity, the subscript k will be dropped from now on. The original model parameter is related to the transformed parameter as

$$m = \frac{a + b\exp(nx)}{1 + \exp(nx)}; \qquad -\infty < x < \infty. \tag{5}$$

Considering the relation (Abramowitz and Stegun 1972)

$$\tanh^{-1} z = \frac{1}{2}\ln\left(\frac{1+z}{1-z}\right), \tag{6}$$

equations (4) and (5) can be rewritten using a hyperbolic tangent function as

$$x = \frac{2}{n}\tanh^{-1}\left(\frac{2m - b - a}{b - a}\right) \tag{7}$$

and

$$m = \frac{b - a}{2}\tanh\left(\frac{nx}{2}\right) + \frac{a + b}{2}, \tag{8}$$

respectively. Thus, the logarithmic transformation in equation (4) is equivalent to the inverse hyperbolic tangent transformation in equation (7).

When $n = 1$, equation (4) becomes the simple logarithmic transformation in equation (1). When $n = 2$, one can easily derive equation (2) from equation (8) and equation (3) from equation (5). This means that the two nonlinear transformations in equations (2) and (3) are one and the same. Consequently, the transformation in equation (4) or (7) can be regarded as a unified expression for lower and upper bounding constraints on model parameters.

Equation (8) clearly shows the shape of transformation functions; the hyperbolic tangent function in the transformation is bounded between -1 and 1 (Abramowitz and Stegun 1972), and so m is between a and b. The graphs

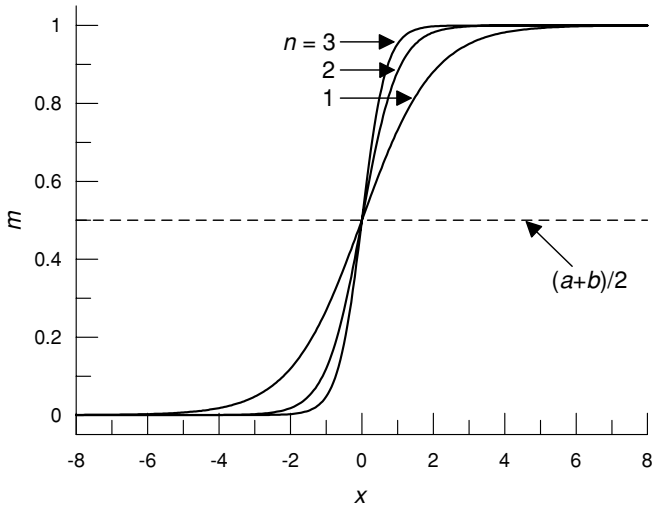

Figure 1. Graph of the logarithmic or inverse hyperbolic tangent transformations, given by equation (3) or (6). The example shows the values of m are bounded between $a = 0$ and $b = 1$.

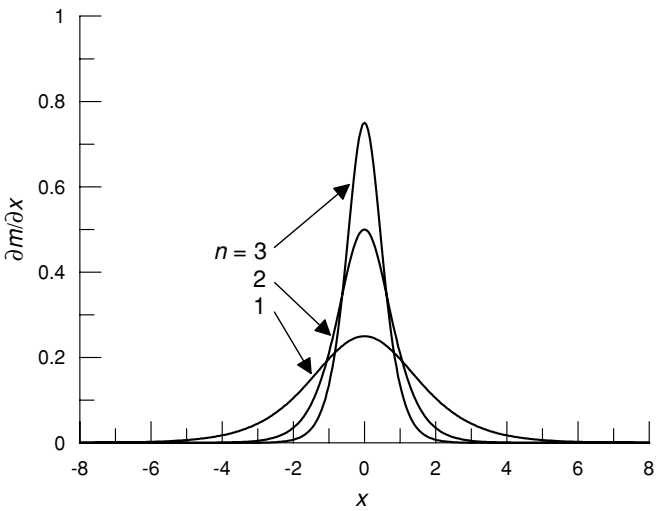

Figure 2. Graph of the derivatives of m with respect to x for $n = 1$, 2 and 3 when the interval $b - a = 1$.

in figure 1 exemplify the transformation types for $n = 1$, 2 and 3. One can observe linear behaviour of transformation functions when the unbounded parameter has values in the vicinity of zero. The gradient of the bounded parameter is maximum at $x = 0$ for $m = (b + a)/2$, the mean of bounds (a, b), and becomes steeper as n increases.

Note that the constant n is not limited to integer values. Common logarithms are often used in one-dimensional (1D) electrical and EM problems (e.g. Constable *et al* 1987), and can be effective in allowing for a wider range of model parameters in inversion than natural logarithms. If the base for logarithms is changed to 10 (common logarithms), equation (1) is modified as

$$x = \log_{10}\left(\frac{m-a}{b-m}\right). \tag{9}$$

Since equation (9) is rewritten as

$$x = \frac{1}{\ln 10}\ln\left(\frac{m-a}{b-m}\right), \tag{10}$$

one can see that equation (9) is also a special case of the unified formula (4), where $n = \ln 10$ (≈ 2.3).

Differentiating equation (5) or (8) with respect to x yields

$$\frac{\partial m}{\partial x} = \frac{n(b-a)\exp(nx)}{[1+\exp(nx)]^2} = \frac{n(b-a)}{4}\operatorname{sech}^2\left(\frac{nx}{2}\right). \tag{11}$$

Substituting equation (4) into equation (11), we obtain

$$\frac{\partial m}{\partial x} = \frac{n(b-m)(m-a)}{b-a}. \tag{12}$$

The hyperbolic secant function in equation (11) is always positive and bounded between 0 and 1. The derivative of m with respect to x is a function of n as well as $b - a$, the interval between the lower and upper limits, and achieves its maximum value of $n(b - a)/4$ when $x = 0$ for $m = (b + a)/2$. The shape of the derivative function is similar to a normal Gaussian distribution as shown in figure 2, and becomes sharper as n increases while maintaining its area to be constant ($= b - a$). In contrast, setting $n < 1$ in the new transformation function yields smaller derivatives compared to the conventional ones ($n = 1$, 2 or 2.3). At the same time, the derivative function increases as $b - a$ increases. This means that m is constrained more tightly to $(b + a)/2$ with an increase of $b - a$. Such constraint becomes stronger when $n > 1$, whereas it becomes weaker when $n < 1$.

Using the derivative function, it is easy to recast the cost functional gradient in terms of the transformed variable as (Kim *et al* 1999, Commer and Newman 2008)

$$\frac{\partial \phi}{\partial x} = \frac{\partial \phi}{\partial m}\frac{\partial m}{\partial x}, \tag{13}$$

where ϕ is the cost functional to be minimized. Once the model increment δx is obtained, initial transformed and original parameters, x_0 and m_0, are updated as

$$x^{\text{updated}} = x_0 + \delta x, \tag{14}$$

and

$$m^{\text{updated}} = \frac{a(b-m_0) + b(m_0-a)\,e^{n\,\delta x}}{(b-m_0) + (m_0-a)\,e^{n\,\delta x}}, \tag{15}$$

respectively.

4. Crosswell tomography

To test the new transformation function on model parameters in inversion, we have selected a synthetic model used in Kim *et al* (2004). The model consists of two cylindrically symmetric bodies, one conductive (10 Ω m) and the other resistive (1000 Ω m), in a whole space of 100 Ω m as shown in figure 3. As an inversion algorithm, we use a smoothness-constrained Gauss–Newton minimization approach described in Kim *et al* (2003, 2004). They applied a localized nonlinear (LN) approximation of integral equation (IE) solutions to inverting borehole EM data using a 2D cylindrically symmetric model. When the LN approximation is applied to the cylindrically symmetric model with a vertical magnetic dipole

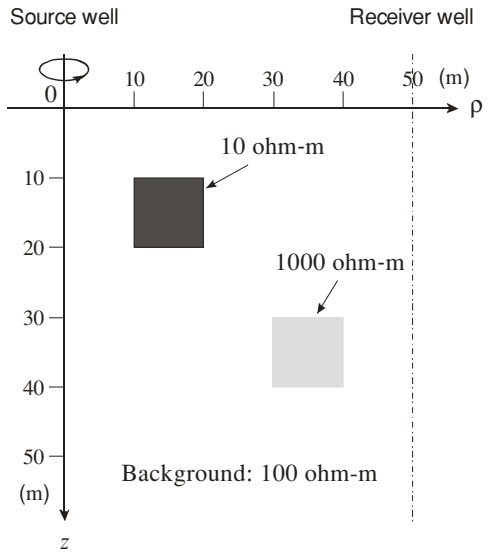

Figure 3. A 2D cylindrically symmetric model used to generate synthetic data for inversion test (redrawn from Kim *et al* 2004). Two rings of 10 Ω m and 1000 Ω m, separated vertically by 10 m, are located in a whole space of 100 Ω m. The upper and lower bodies are horizontally 10 m and 30 m away from the source borehole, respectively.

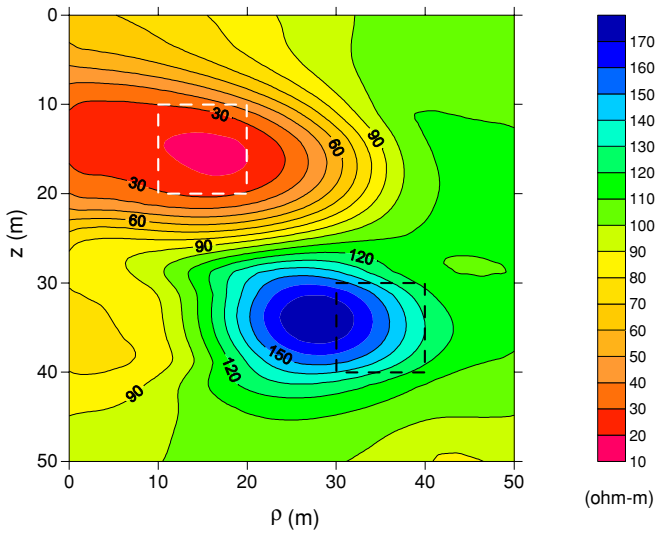

Figure 4. A resistivity image of the two bodies reconstructed from inversion of the synthetic crosswell EM data after eight iterations. The bound constraints with $n = 2$ are used during inversion. The lower and upper bounds of 2 and 5000 Ω m are applied to the whole inversion blocks.

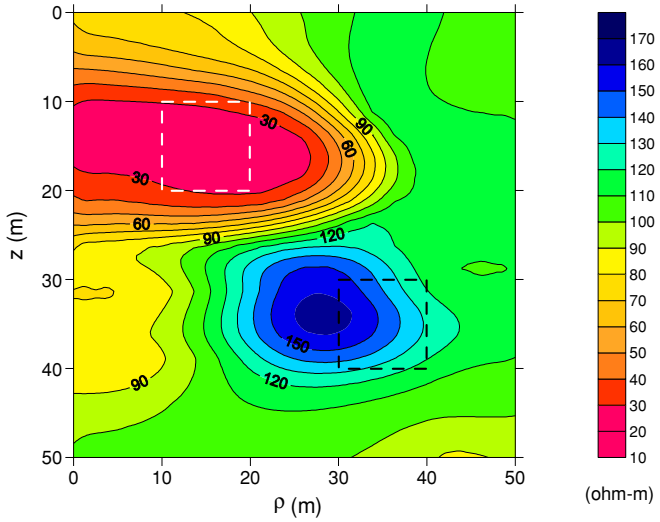

Figure 5. A resistivity image after eight iterations when the bound constraints with $n = 0.5$ are used during inversion. The lower and upper bounds applied to the whole inversion blocks are the same as in figure 4.

source, it works well because the azimuthal electric fields are scalar and continuous everywhere. The inversion technique seeks the minimum structure solution that best reproduces the data to solve the ill-posed problem. One of the most important steps in the regularized inversion is the selection of a proper regularization parameter for stability. The LN solution provides an efficient way to select the proper regularization parameter because Green's functions are repeatedly re-usable at each iteration (Kim *et al* 2003, 2004).

A finite-element scheme (Lee *et al* 2005) is used to generate synthetic data, which are susceptible to different types of numerical errors from the IE technique. Using a vertical magnetic dipole as a source, vertical magnetic fields are computed at three frequencies: 2.5, 10 and 20 kHz. Three per cent Gaussian noise is added to the synthetic data prior to inversion. The inversion domain consists of 672 ($= 24 \times 28$) square blocks, and the size of each block is 2.5 m × 2.5 m. The initial model is a homogeneous 60 Ω m whole space. Constant lower/upper bounds of 2/5000 Ω m are applied to all model parameters.

We compare $n = 2$ and 0.5 through inverting the synthetic data. The inversion process was quite stable, and the rms misfit decreased from an initial guess of 19.13 to 0.032 and 0.031 after eight iterations for $n = 2$ and 0.5, respectively. The final rms misfits are considered to be nearly a target misfit level because the artificial noise added to the synthetic data was 3%. After eight iterations, the two bodies are clearly imaged as shown in figures 4 and 5, but the images are smeared both horizontally and vertically, mainly due to model smoothness imposed for stabilizing the inversion. The recovered resistivity is found to be almost the same in the conductive body, but is largely underestimated in the resistive body. Furthermore, the resistive body is imaged slightly left of the original position in the resistivity sections. It is well known that induction measurements are more sensitive to conductive objects than to resistive ones (e.g. Abubakar *et al* 2008), and that the horizontal resolution is much poorer than the vertical resolution in crosswell EM tomography (e.g. Alumbaugh and Morrison 1995).

The reconstructed resistivity image varies with the constant n, which controls the model parameter gradient with respect to the transformed variable. In particular, the contour interval between the two bodies differs with n. Larger n is useful to produce a relatively smooth resistivity variation as shown in figure 4, whereas smaller n yields squeezed

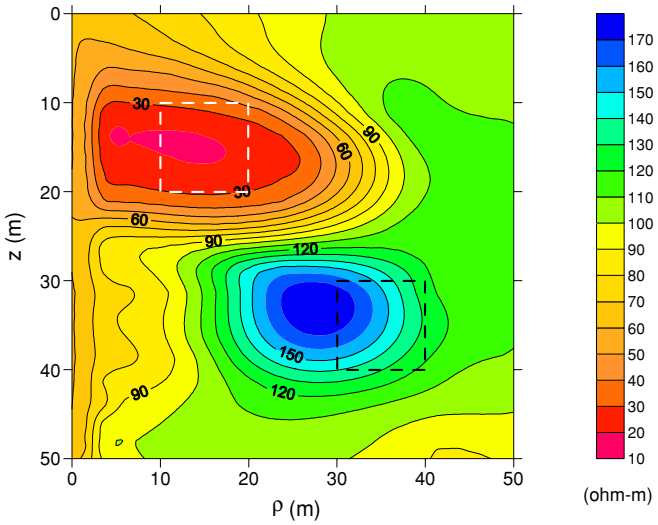

Figure 6. A resistivity image after eight iterations when the bound constraints with $n = 1$ are used during inversion. The lower and upper bounds of 50 and 200 Ω m are applied to the nearest inversion blocks from the source well.

contour intervals between the anomalies as in figure 5. The conventional transformation functions are equivalent to $n = 1$ (e.g. Kim *et al* 1999) and $n = 2$ (Commer and Newman 2008, Abubakar *et al* 2008) in the unified formula.

In figures 4 and 5, a conductive overshoot occurs at depths of 10–20 m near the source well. If *a priori* information such as logging data is available, we may apply tighter bounds to specific inversion blocks. Figure 6 shows the result of another inversion experiment, where we used $n = 1$ and set the resistivity of the nearest blocks from the source well to be bounded between 50 and 200 Ω m. The target resistivity of these blocks is 100 Ω m. From the illustration, one can see that the conductive overshoot at depths of 10–20 m is largely reduced. While the overall resistivity image is similar to those in figures 4 and 5, the contour interval between the two anomalies is a medium of the two figures ($n = 2$ and 0.5).

5. Discussion and conclusions

As electrical and EM inverse problems are ill-posed, *a priori* information about unknown parameters are of particular importance for the inversion process. In this paper, we described a unified transformation function for lower and upper bounding constraints on model parameters to introduce *a priori* constraints. This scheme converts a constrained inverse problem to an unconstrained type. Using lower and upper bounding constraints, model parameter updates during the inversion process are restricted such that unrealistic results are suppressed.

The advantage of this type of transformation is that it can produce sharper image rendering if tight bounds are selected from *a priori* information, as Commer and Newman (2008) demonstrated in nonlinear conjugate gradient inversion of synthetic and field EM data. Cardarelli and Fischanger (2006) also illustrated in their synthetic example that the use of bound constraints can make the procedure of smoothness-constrained least-squares inversion less dependent on damping factors. Whatever minimization procedures are employed, these studies clearly show that the use of bound constraints helps improve the model reconstruction and facilitates the inversion procedure. However, if the bounds are too restrictive, then they may act as barriers in the minimization process and prevent reaching acceptable data fits (Pedersen 2004, Commer and Newman 2008).

The unified transformation function, which is expressed as a logarithmic or inverse hyperbolic tangent function, proposed in this paper is quite general. The conventional transformation functions introduced in Kim *et al* (1999), Commer and Newman (2008), and Abubakar *et al* (2008) are included in the new transformation function as special cases. With the cost functional gradient with respect to the transformed variable, equation (13), one can apply an inversion algorithm directly to the transformed problem, which implicitly enforces the bound constraints. The conventional transformation function ($n = 1$ or 2) has a smaller model parameter gradient with respect to the transformed variable than the common logarithmic transformation ($n = \ln 10 \approx 2.3$). In contrast, the constant n can be set to less than 1 for smaller model parameter gradients. Thus the model parameter gradient is easily controlled with the constant n in the new transformation function.

To test the characteristics of bound constraints, we applied a regularized Gauss–Newton inversion technique to synthetic crosswell EM data. The inversion experiment showed that the conventional transformation function ($n = 2$) is effective for reconstructing a relatively smooth resistivity distribution as shown in figure 4. In contrast, the smaller constant n yields an image with more squeezed contour intervals between the anomalies (figure 5). Although the synthetic examples showed that acceptable resistivity images can be reconstructed with smooth convergence, solution non-uniqueness remains a formidable problem.

The interval between the parameter bounds reflects the reliability of *a priori* information, which may be estimated through well logging and surface geological surveys. An example of tight bounds utilizing logging information was given to demonstrate better recovery of resistivity distribution from inversion as in figure 6. It is therefore important that *a priori* information is incorporated in the imaging process to limit the class of solutions to geologically meaningful ones.

Acknowledgments

This work was supported by the Korea Research Foundation grant (KRF-2008-013-D00159). We would like to thank two anonymous reviewers for their valuable comments in improving the quality of this manuscript.

References

Abramowitz M and Stegun I A 1972 *Handbook of Mathematical Functions* (New York: Dover)

Abubakar A, Habashy T M, Druskin V L, Knizhnerman L and Alumbaugh D 2008 2.5D forward and inverse modeling for

interpreting low-frequency electromagnetic measurements *Geophysics* **73** F165–77
Alumbaugh D L and Morrison H F 1995 Theoretical and practical considerations for crosswell electromagnetic tomography assuming a cylindrical geometry *Geophysics* **60** 846–70
Cardarelli E and Fischanger F 2006 2D data modelling by electrical resistivity tomography for complex subsurface geology *Geophys. Prospect.* **54** 121–33
Commer M and Newman G A 2008 New advances in three-dimensional controlled-source electromagnetic inversion *Geophys. J. Int.* **172** 513–35
Constable S C, Parker R L and Constable C G 1987 Occam's inversion: a practical algorithm for generating smooth models from electromagnetic sounding data *Geophysics* **52** 289–300
Kim H J, Lee K H and Wilt M 2003 A fast inversion method for interpreting borehole electromagnetic data *Earth Planets Space* **55** 249–54
Kim H J, Song Y and Lee K H 1999 Inequality constraint in least-squared inversion of geophysical data *Earth Planets Space* **51** 255–9
Kim H J, Song Y, Lee K H and Wilt M 2004 Efficient crosswell EM tomography using localized nonlinear approximation *Explor. Geophys.* **35** 51–5
Lee K H, Kim H J and Uchida T 2005 Electromagnetic fields in a steel-cased borehole *Geophys. Prospect.* **53** 13–21
Mackie R L and Madden T R 1993 Three-dimensional magnetotelluric inversion using conjugate gradients *Geophys. J. Int.* **115** 215–9
Newman G A and Alumbaugh D L 2000 Three-dimensional magnetotelluric inversion using non-linear conjugate gradients *Geophys. J. Int.* **140** 410–24
Pedersen L B 2004 Determination of the regularization level of truncated singular-value decomposition inversion: the case of 1D inversion of MT data *Geophys. Prospect.* **52** 261–70
Song Y and Kim J-H 2008 An efficient 2.5D inversion of loop–loop electromagnetic data *Explor. Geophys.* **39** 68–77
Tikhonov A N and Arsenin V Y 1977 *Solutions of Ill-Posed Problems* (Washington, DC: Winston)
Ueda T and Zhdanov M S 2009 Marine CSEM inversion based on the regularized conjugate gradient method and EM migration *Butsuri-Tansa* **62** 295–306 (in Japanese with English abstract)